KAMPALA INTERNATIONAL UNIVERSITY

KIU
Journal of Science, Engineering and Technology

KJSET Research Article

Energy management in cooling system using hybrid optimization clustering technique

Elnazeer Ai Hamid Abdalla[1,2], Ahmed Mohammed Ishag[1,3], Mohammed Elnour A/Alla[1,4], Tamador Elkhansaa .J Mohamed[1] Saadelnour Abdueljabbar Adam[1,3] , Bubu Pius Erheyovwe [1] , and Akankunda Joan [1]

Dept. of Electrical, Telecommunication & Computer/Biomedical Engineering, Kampala International University Uganda[1]
Department of Electrical and Electronic Engineering, University of Bahri, 1111 Bahri, Khartoum, Sudan[2]
Department of Electrical and Electronic Engineering, University of Nyala, Nyala, Sudan[3]
School of Electronics Engineering, Sudan University of Science and Technology (SUST), Khartoum, Sudan[4]
hamidelnazeer@kiu.ac.ug[12], ahmed.ishag@kiu.ac.ug[1,3], mohammed@kiu.ac.ug[1,4], tamador.jaber@kiu.ac.ug[1] , saadelnour@kiu.ac.ug[1,3], bubupiu.e@kiu.ac.ug[1] , joanakankunda@kiu.ac.ug[1]

Corresponding Author: hamidelnazeer@kiu.ac.ug[1,2]

Paper history:
Received 13th November 2024
Accepted in revised form 13th December 2024

Keywords
Cooling energy; energy consumption; Fuzzy subtractive clustering (FSC); Accelerated particle swarm optimization (APSO); Cooling performance.

Abstract

Malaysia is situated in Southeast Asia, close to the equator, and as a result of its position, it has hot and humid weather. Because of the impact of the high ambient temperature, more than 50% of the building's energy is used to meet the cooling load demand. Reducing energy consumption in cooling systems without compromising cooling load demand is still an issue to manage. Numerous research studies have been conducted on cooling load demand and its power usage in order to regulate energy consumption and cooling load. These studies have included fuzzy c-mean (FCM) and fuzzy subtractive clustering (FSC) have been involved in cooling systems. As a result, when it comes to deciding how many clusters to use and deploying big data, both FCM and FSC are constrained. This work proposes accelerated particle swarm optimization (APSO) and FSC techniques to achieve this. By adjusting the cluster radius of the FSC-based APSO algorithm. To tune and adjust the cluster radius, a proportional-integral (PI) controller is adopted. The main objective of the APSO is to fine-tune the data clustering parameters. The outcome of the proposed FSC-APSO based PI technique is to identify the input-output dataset for evaluating electricity usage and cooling load demand. The energy usage and load demand in this work are evaluated based on the influence of ambient temperature and relative humidity. The results show that the FSC-APSO technique reduces energy consumption by 10% without compromising comfort-cooling demand. The result is validated using actual data obtained from Latexx Manufacturing Sdn Bhd, Malaysia.

Nomenclature and units

1.0 Introduction

Malaysia is ranked at 52 on the climate change index. It evaluates 90% of global CO2 emissions of 57 countries (Shaikh et al., 2017). Cooling buildings of residential and commercial sectors consume (10 – 60) % of electricity by chiller plants (Chong, Ni, Ma, Liu, & Li, 2015). The cooling demand in buildings is high, if the climate is humid-hot throughout the year (Shaikh et al., 2017). The hot weather requires high load demand that results in more energy consumption (Patterson, 2008; Yi-Ling, Hai-Zhen, Guang-Tao, & Jun, 2014). Thus, energy conservation without compromising demand is an issue in cooling system. The cooling load demand has a direct effect on the energy consumption especially when the weather condition is humid and hot. Optimization techniques can be used to manage demand that significantly reduces energy usage (Abdalla et al., 2016; Hamid, Nallagownden, Nor, & Muthuvalu, 2014; Nallagownden, Abdalla, Nor, & Romlie, 2017; Radeerom & Tharathanmathikorn, 2015), and water consumption (Maiolo, Mendicino, Pantusa, & Senatore, 2017; Mala-Jetmarova, Sultanova, & Savic, 2018). Numerous studies have been used to solve the clustering problem (Hamid Abdalla, Nallagownden, Mohd Nor, Romlie, & Hassan, 2018), but it remains open for many ideas to come to achieve energy conservation without compromising load demand. In (Hamid Abdalla et al., 2018), FSC and APSO algorithms carried out separately to investigate the cooling behavior and they both are achieved good results. A recent study in (Abdalla et al., 2023), showed a reduction in energy usage while maintaining cooling demand. The authors did not consider the weather data such as ambient temperature and relative humidity. However, clustering fuzzy suffers from a lot of issues when implementing big data (ABDALLA, 2020). To address the issues such as big data when it implemented results in a computation time burden. Also, the number of clusters is not easy to assume, and the radius of the cluster has an effect on the selection of cluster numbers (Nallagownden, Abdalla, & Nor, 2020). This work focuses on developing a new technique intended to be applied to overcome the drawbacks of FSC with APSO by tuning the parameters of the FSC algorithm. In that regard, a hybrid of FSC and APSO is proposed to quantify the best data-points in order to maintain cooling demand and reduce energy consumption (usage). The remaining part of the paper is organized as follows: Section 2 details the methodology (method) employed in this paper, while Sections 3 and 4 present the simulation results, discussion, and analysis. Finally, in Section 5, we summarize paper conclusions.

2.0 Materials and Data Collection

The methodology is investigated in cooling water plants serving an industrial building at Latexx Manufacturing Sdn Bhd, Perak Malaysia. It consists of 5 chillers, 10 water pumps, and 3 cooling towers shown in Figure 1. Each chiller has a 740 kW nominal cooling capacity by evaporator. This cooling capacity consumes electricity of 140 kW. Each chiller provides a chilled water of 105 m^3/h (29.4 kg/s) to the building at 6.5 °C. Then, it returns to chillers once again at 12.5 °C. Figure 2 (a, b) shows the energy usage, cooling load, and the return temperature (T_{CHWR}). It is obvious that when the T_{CHWR} is high due to the hot / high ambient temperature / humidity, it would result in consuming more energy and the cooling demand

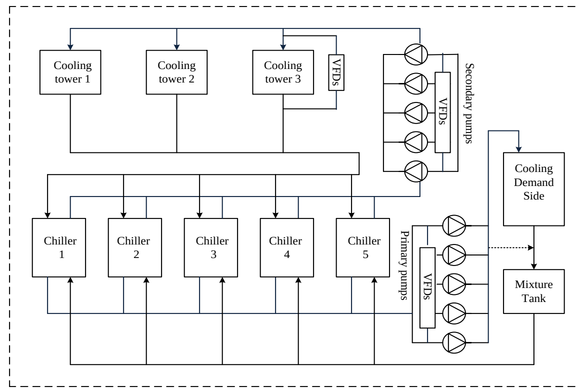

Figure 1 A block diagram of CHP system

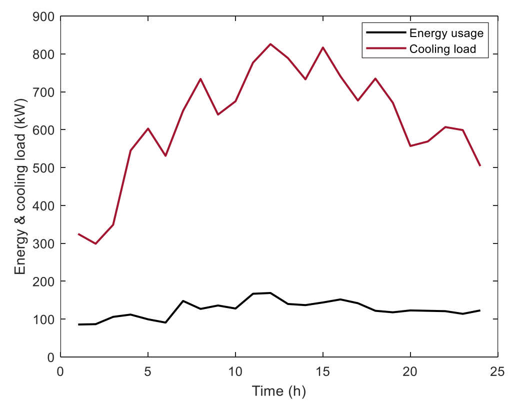

Figure 2 (a) One chiller cooling load and energy consumption, May 2015 (Nallagownden et al., 2020)

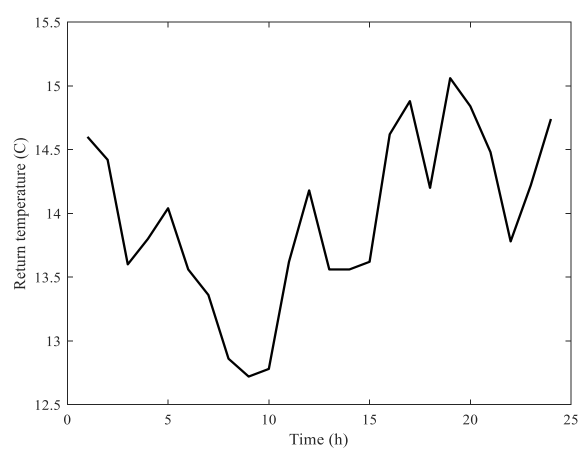

Figure 2 (b) Chilled-water return temperature, May 2015 (Nallagownden et al., 2020)

The temperature ‘T_{CHWR}’ increases due to the weather condition and consequently, the chilled water systems consume more energy to keep cooling demand satisfied. The humid-hot weather has a negative impact that varies the need for cooling demand dramatically. Figure 3 shows the flow rate, return temperature, ambient temperature and relative humidity. These data are used as inputs to evaluate the cooling demand with a minimum energy. The input data ranged (*min* – *max*) as depicted in Table 1.

Table 1 Input data obtained from, (Nallagownden et al., 2020)

Input data	*symbol*	*values*
Temperature difference (°C)	ΔT_{CHW}	5.5 – 9
Chilled water flow (kg/s)	M_{CHW}	10 – 29
Temperature difference (°C)	T_{AMB}	24 – 36
Ambient humidity (%)	R_H	46 – 100

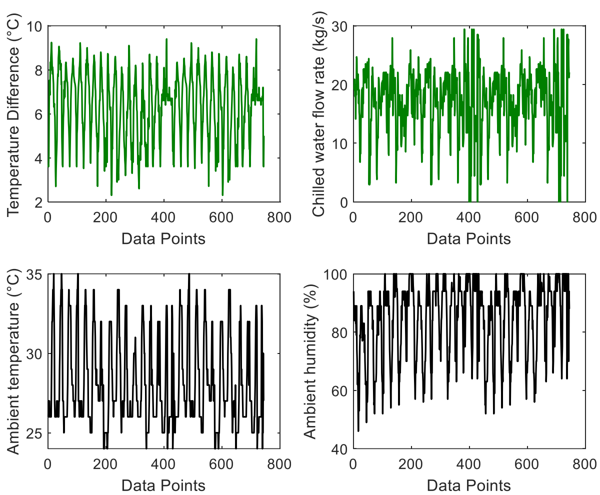

Figure 3 System data and Taiping monthly ambient temperature and humidity, May 2015 (Nallagownden et al., 2020)

3.0 The Proposed Method

3.1. Proposed Model System

The amount of chilled water flow rate can be determined based on the *m*th number of chillers as,

$$M_{CHW} = m \sum_{m=1}^{M} M_{CHW} \tag{1}$$

The chilled water return temperature of *i*th datasets ($T_{CHWR,i}$) has a direct effect on the amount of chilled water flow which will be influenced by the weather condition as,

$$T_{CHWR,i} = \begin{bmatrix} q_1 \\ q_2 \\ \vdots \\ q_n \end{bmatrix}^T \begin{bmatrix} C_{ij} \end{bmatrix} + \begin{bmatrix} q_{01} \\ q_{02} \\ \vdots \\ q_{0n} \end{bmatrix} \tag{2}$$

where $\{C_{ij}\}$: is the matrix equation for each number dataset (i) and each number of cluster (j), it can be written as,

$$\begin{bmatrix} C_{ij} \end{bmatrix} = \begin{bmatrix} \Delta T_{CHW1} & M_{CHW1} & T_{AMB1} & R_{H1} \\ \Delta T_{CHW2} & M_{CHW2} & T_{AMB2} & R_{H2} \\ \vdots & \vdots & \vdots & \vdots \\ \Delta T_{CHWn} & M_{CHWn} & T_{AMBn} & R_{Hn} \end{bmatrix}^T \tag{3}$$

where n: number of datasets, M_{CHW}: flow rate of chilled water, $\Delta T_{CHW} = (T_{CHWR} - T_{CHWS})$: difference between return and supply temperature of chilled water, T_{AMB}: ambient temperature, and R_H: ambient humidity. The flow rate of chilled water and its temperature difference both are used to evaluate the amount of chilled water capacity (kW) to provide comfort level as,

$$Q_W = 4.197 M_{CHW_i} \left[\sum_{m=1}^{M} T_{CHWR,i} - T_{CHWS,i} \right] \tag{4}$$

The chillers performance may not be operated under standard design condition due to the weather condition, especially when the ambient temperature is hot (Lee, Chen, & Wu, 2009). T_{CHWR} has an impact on the chiller's consumption due to its influenced by outdoor temperature (Patterson, 2008; Yi-Ling et al., 2014). The energy consumption of chilled water systems have been expressed with temperature difference 'ΔT_{CHW}' (Deng et al., 2015), and with flow rate and temperature 'M_{CHW} & ΔT_{CHW}' (Hamid Abdalla et al., 2018). Thus, energy consumption can be expressed as,

$$P_E = a_0 M_{CHW_i} \left[\sum_{k=1}^{4} T_{CHWR_i} - T_{CHWS_i} + b_0 \right] \tag{5}$$

where q_{i1}, q_{i2}, q_{i3}, q_{i4}, q_{i0} are coefficient of the approximate modeling data. Table 2 shows the values of coefficients to calculate the amount of chilled water capacity. The mathematical model in this section is compared with the fundamental equations as shown in **Appendix A**.

Table 2 The coefficient of the approximate measured data

coeff.	q_{1i}	q_{2i}	q_{3i}	q_{4i}	q_{0i}	a_0	b_0
value	1.028	.0084	.0003	.0074	5.83	0.75	7.7

3.2. Hybrid of FSC-APSO Technique

This section describes in detail the proposed technique, Fig. 4 shows the main steps to classify data to assess cooling load and electricity consumption. Firstly, it starts with the identification of input data and the number of clusters and then converting to fuzzy rules with FSC technique. Secondly, the FSC is optimized by APSO to enhance its performance.

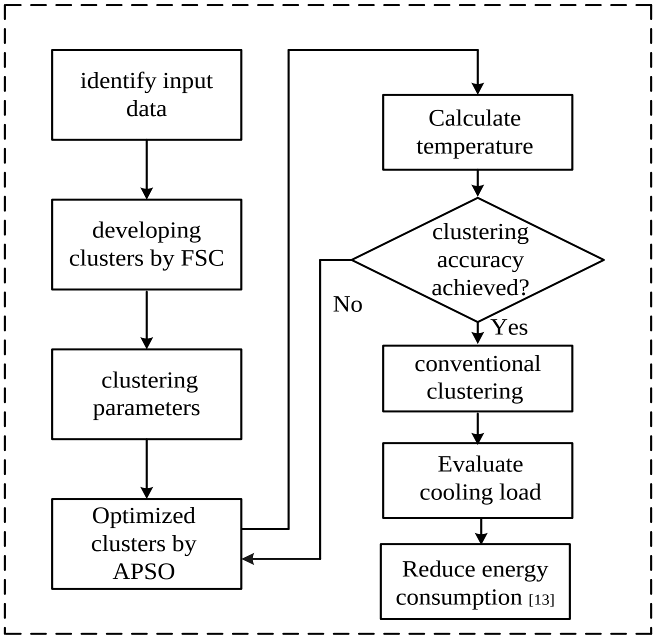

Figure 4. Flow Chart of implementation of clustering technique

3.2.1. FSC Technique

Air-conditioning cooling systems can be controlled and managed with fuzzy systems (Rezeka, Attia, & Saleh, 2015). One fuzzy application that has recently emerged as a leading method for classifying large data FSC which may be used in a variety of applications to investigate various objective (Fong, Wong, & Vasilakos, 2015; Hamid Abdalla et al., 2018; Siddiqi & Sait, 2017). By examining the collected data using particular structures to find the best point among the data points, FSC is used to estimate the data clustering numbers, by searching the cluster center of data with specific structures to select the best point among data points. Let, x_1, x_2,…, x_n represent inputs {ΔT_{CHW}, M_{CHW}, T_{AMB}, R_H} and each has the potential to be cluster center C_1, C_2,…, C_k. Thus, the density of i^{th} data points can be expressed as (Hamid Abdalla et al., 2018),

$$y_l = \sum_{l=1}^{4} e^{\left\{-\frac{\|x_l - C_k\|^2}{(r_a/2)^2}\right\}} \qquad (6)$$

where r_a is the cluster neighborhood radius (0 *to* 1), $\rho = 4/r_a^2$, and $\|x_l - C_k\|$ is the Euclidean distance. The r_a has an impact on data density and Euclidean distance. Let C_k to be found in the clustering group of x_l, this cluster provides a fuzzy expressed as,

$$Rule(R) = \{if\ x_i\ is\ \pi_{jk}\}, then\ \{Y_j = C_k\} \qquad (7)$$

where x_j is the l^{th} input feature and π_{ij} is the membership function (MF) in the rule associated with the l^{th} input. The MF is written by,

$$\pi_{ij}(x_j) = e^{-\rho\|x_j - c_i\|^2} \qquad (8)$$

Each input has a degree of participation in every fuzzy set, based quantitatively on MF. Figure 5 depicts fuzzy sets and each input data has four fuzzy rules. The fuzzy rules have different value for each input; low (L), medium low (ML), medium high (MH), and high (H) value.

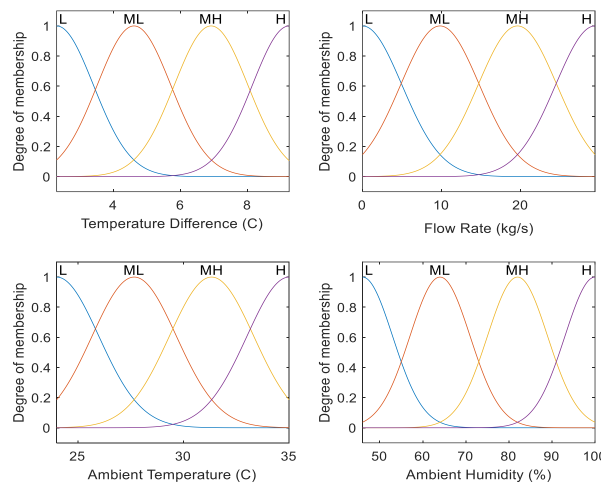

Figure 5. Fuzzy sets and memberships function of fuzzy inference system (FIS), (Nallagownden et al., 2020)

The MF of the fuzzy set has a degree ranging from 0 to 1. The MF for the fuzzy set has a degree ranging from 0 to 1. The MF has grades of inputs with the Gaussian function, which is expressed by,

$$\mu_{ij}(x_j) = e^{\left\{\frac{-[x_j - c_i]^2}{2\sigma_i^2}\right\}} \qquad (9)$$

where $\sigma^2 = 1/2\rho$, c_i is the data mean/center of k^{th} cluster, and σ_i is the standard deviation of each MF (Hamid Abdalla et al., 2018). In Figure 5, each input fuzzy linguistic has 4 different sets as low (L), medium-low (ML), medium-high (MH), and high (H) value. The MF parameters in Eq. (14) were calculated based on inputs experimental data by the procedure of FSC. When FSC is performed, the consequence of the fuzzy rule with the highest degree of fulfilment is selected to be the required output class (centroid of each fuzzy rule).

3.2.2. Accelerated particle swarm optimization

Accelerated Particle swarm optimization (APSO) is a version of the PSO algorithm, and it was suggested to overcome the limitations of FSC (Hamid Abdalla et al., 2018). The fuzzy sets of inputs have 4 MFs optimized by FSC-APSO1, by FSC-APSO2, and by FSC-APSO3, and the parameters of fuzzy of each MF C_{ij} and σ_{ij} shown in Figure 6.

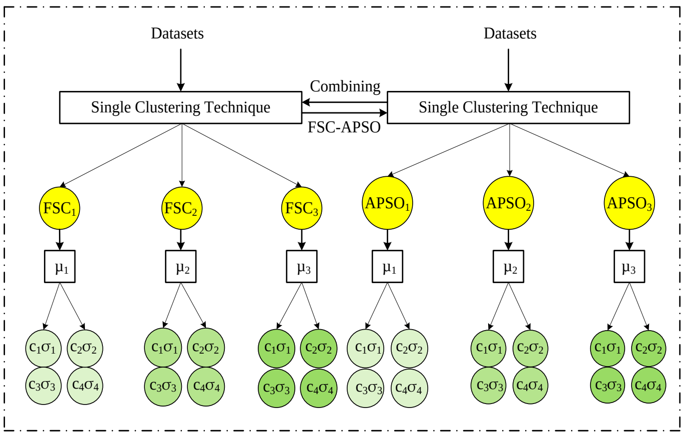

Figure 6. The flow chart of fuzzy encoding with FSC-APSO tecnique

The parameter sets of MF degree for each generating fuzzy rule are assigned particle position. First, initialize each MF parameter and encoded into particles N_p (i = 1, 2, …, 50). Create 16 particle vectors of fuzzy rules for each input and the particle vectors (C_{ij}, σ_{ij}), then we determine the bounds of each input. After fuzzy rules structure created, the grid partitioning is used to locate the C_{ij} and σ_{ij} with Guassian function. The inputs are partitioned, and each value is chosen randomly within its respective range after calculating the data density in Eq. (6). Then, the vectors are assigned based on particle velocity (V_{ij}) and its position (λ_{ij}),

$$V_{ij}^{(\tau+1)} = V_{ij}^{(\tau)} + \alpha r_{ij} + \beta\left(gbest_j^{(\tau)} - \lambda_{ij}^{(\tau)}\right) \tag{10}$$

$$\lambda_{ij}^{(t+1)} = \lambda_{ij}^{(\tau)}(1-\beta) + \beta\left(gbest_j^{(\tau)}\right) + \alpha r_{ij} \tag{11}$$

where gbest is the global for best solution so far for all particle Np, r_{ij} is the random number (0, 1), α and β are the acceleration parameters typically ≤ 1 (Hamid Abdalla et al., 2018).

From Eq. (6), the cluster radius is selected from α and β as,

$$r_{ai} = 2\left[\frac{\alpha_k \beta_k}{\alpha_k + \beta_k}\right] * rand_n \tag{12}$$

Each membership has a center point influenced by r_a and each particle *i* generates membership grades of inputs. The center point of each MF is chosen with the goal of distributing the MFs throughout the whole range, and thus the range is partitioned and then each center value is chosen randomly within its respective partition. Here, the 'λ_{ij}' of C and σ assigned based on MF partition, and 'r_a' of each input is assigned as position vectors as,

$$\lambda_{ij} = \{r_{a1}, r_{a2}, \dots, r_{an}\},\ j^{th} = 1, 2, 3, 4 \tag{13}$$

The r_a value is updated by the change of r_a (Δr_a) with the accelerated particle and therefore, the 'r_a' of each input is assigned as position vectors as,

$$\begin{aligned}\lambda_i &= \{\lambda_{i1}, \lambda_{i2}, \dots, \lambda_{iN_P}\} \\ &= \{r_{ai1} \mp \Delta r_{ai1},\ r_{ai2} \mp \Delta r_{ai2} \dots,\ r_{ain} \mp \Delta r_{ain}\}\end{aligned} \tag{14}$$

where; Δr_{aij} is used to tune r_a that is resulted in optimal data points (cluster centers). The evaluation for particle's vectors λ_i is calculated according to Eq. (6). The swarm (N_p = 50) of each particle *i* at iteration τ =50 for cluster sets express as,

$$if\ \tau_i\ then\ \lambda_i = (r_{ai} \mp \Delta r_{ai})$$

$$\leftrightarrow \left\{\begin{array}{ll}
\tau^1 = 0, & \lambda_1^1(0), \lambda_2^1(0), \lambda_3^1(0), \dots, \lambda_{50}^1(0) \\
\tau^1 = 1, & \lambda_1^1(1), \lambda_2^1(1), \lambda_3^1(1), \dots, \lambda_{50}^1(1) \\
\tau^1 = 2, & \lambda_1^1(2), \lambda_2^1(2), \lambda_3^1(2), \dots, \lambda_{50}^1(2) \\
 & \vdots \\
\tau^1 = 50, & \lambda_1^1(50), \lambda_2^1(50), \lambda_3^1(50), \dots, \lambda_{50}^1(50) \\
 & \dots \\
 & \dots \\
\tau^2 = 0, & \lambda_1^2(0), \lambda_2^2(0), \lambda_3^2(0), \dots, \lambda_{50}^2(0) \\
\tau^2 = 1, & \lambda_1^2(1), \lambda_2^2(1), \lambda_3^2(1), \dots, \lambda_{50}^2(1) \\
\tau^2 = 2, & \lambda_1^2(2), \lambda_2^2(2), \lambda_3^2(2), \dots, \lambda_{50}^2(2) \\
 & \vdots \\
\tau^2 = 50, & \lambda_1^2(50), \lambda_2^2(50), \lambda_3^2(50), \dots, \lambda_{50}^2(50) \\
 & \dots \\
 & \dots \\
\tau^3 = 0, & \lambda_1^3(0), \lambda_2^3(0), \lambda_3^3(0), \dots, \lambda_{50}^3(0) \\
\tau^3 = 1, & \lambda_1^3(1), \lambda_2^3(1), \lambda_3^3(1), \dots, \lambda_{50}^3(1) \\
\tau^3 = 2, & \lambda_1^3(2), \lambda_2^3(2), \lambda_3^3(2), \dots, \lambda_{50}^3(2) \\
 & \vdots \\
\tau^3 = 50, & \lambda_1^3(50), \lambda_2^3(50), \lambda_3^3(50), \dots, \lambda_{50}^3(50) \\
 & \dots \\
 & \dots \\
\tau^4 = 0, & \lambda_1^4(0), \lambda_2^4(0), \lambda_3^4(0), \dots, \lambda_{50}^4(0) \\
\tau^4 = 1, & \lambda_1^4(1), \lambda_2^4(1), \lambda_3^4(1), \dots, \lambda_{50}^4(1) \\
\tau^4 = 2, & \lambda_1^4(2), \lambda_2^4(2), \lambda_3^4(2), \dots, \lambda_{50}^4(2) \\
 & \vdots \\
\tau^4 = 50, & \lambda_1^4(50), \lambda_2^4(50), \lambda_3^4(50), \dots, \lambda_{50}^4(50)
\end{array}\right\} \tag{15}$$

Since all FSC cluster centres can be further tuned by APSO based on the influencer 'r_a', the initial 'r_a' is simply set between 0.4 – 0.7. The change in cluster radius in Eq. (14) varies in C_{ij} value accordingly. For each iteration τ, a new population is produced, and the old population is replaced to be stored. The new and old populations are compared for each other and the initial positions are created arbitrary according to the all best (gbest) performance. The values of the particle velocity are generated randomly by $v_i(0)$, i =1, 2, 3, … , 50. Then, from Eq. (12), the best 'λ' for the 'r_a' of all particles (gbest) are calculated from Eq. (10) and (11). Figure 7 depicts the flowchart of the FSC-APSO algorithm. The proposed algorithm has been developed in three steps.

- Step 1: data classification and grouping-based FSC clustering technique.
- Step 2: data clustering in step are tuned and optimized by APSO for clustering radius
- Step 3: adjust clustering radiuses using proportional-integral (PI) controller to be ranged between 0.4 – 0.5.

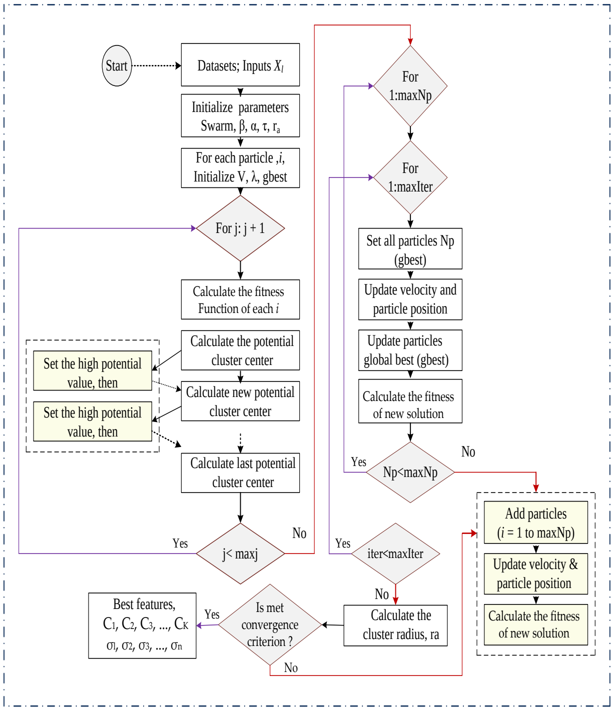

Figure 7. The flow chart of the FSC-APSO technique

To overcome the drawback of FSC, accelerated particle swarm optimization (APSO) is integrated with clustering data-based FSC. From Eq. (12), the cluster radius is selected from α and β as (ABDALLA, 2020). A recent study in (Abdalla et al., 2023) showed that the clustering radiuses ranged between 0.3 to 0.8 give better FSC accuracy and optimal cluster centres. Equation (14) did not achieve the ranged values because random (0, 1). Herein, a proportional-integral (PI) controller will be used to tune the radius of clustering data.

3.2.3. FSC-APSO based PI controller

In this work, proportional integral (PI) controller model in Figure 8 is suggested to tune the radius of clusters to be ranged between 0.4 and 0.5 for efficient outcomes.

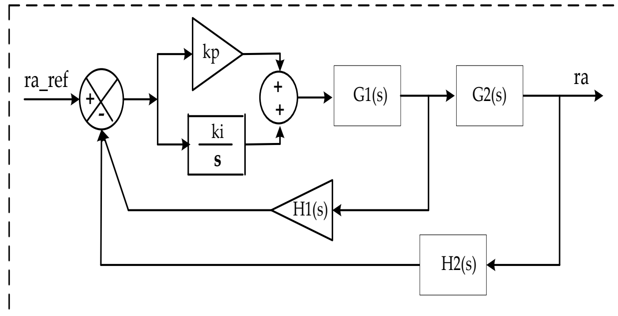

Figure 8. PI controller model for tuning clustering radiuses

The PI model shown in Figure 9, for tuning cluster's radius shows the optimum clustering 0.47, and the parameters of PI model are given in Table 3.

Table 3 The values of PI controller parameters

Parameters	Value
Ø	2.1
k_p	1.5
k_i	0.05 – 0.15

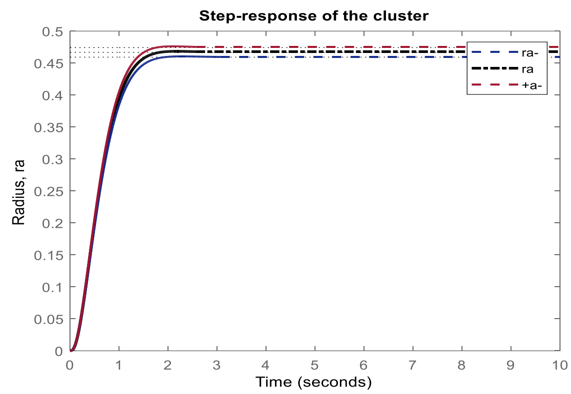

Figure 9. The outcome of PI model for clustering radiuses

3.6. Simulation Parameters

Three scenarios were implemented with clustering data with predefined inputs in Table 4. Let rand = 1 as a reference, then ra is 0.54. We generated three random numbers as 0.87, 0.79, and 0.95 for scenario 1, scenario 2, and scenario 3, respectively.

Table 4 The input parameters of the FSC-APSO technique

Input	Value	Input	Value	Input	Value
Each cluster C_i	186	Iteration	50	radius: r_{a1}, r_{a2}, r_{a3}	0.47, 0.43, 0.51
No. of clusters	4	Swarm	50	Δr_{a1}, Δr_{a2}, Δr_{a3}	0.05, 0.09, 0.01
Random (r_{ij})	0-1	α & β	0.47 & 0.63	$rand_1$, $rand_2$, $rand_3$	0.87, 0.79, 0.95

The first scenario termed as FSC-APSO1 (A1) was implemented when 'r_{a1}' set with 0.47. The second scenario termed as FSC-APSO2 (A2) conducted with 'r_{a2}' tuned to 0.43. The third scenario termed as FSC-APSO3 (A3) was carried out when 'r_{a3}' set to 0.51. Every cluster class has 186 datasets is represented as a center point of 'C_i'. Next, 'C_i' has been assigned to represent datasets and the particle vector for each C_i in the search space is restricted with a minimum and maximum scale. The change in the radius parameter has influenced on the difference between the potential cluster centre 'C_i' and any data-point 'x_i' among 186. Four optimal clustering inputs represent the means (C_{ij}), standard deviations (σ_{ij}), and the output (target) T_{CHWRi} are given in **Appendix B**. The clusters or adjusted fuzzy rules with FSC, FSC-PSO, and FSC-APSO are chosen a suitable cluster center 'C_{ij}' to meet the requirements of cooling load demand. Each cluster represents the distinct operating conditions of the chillers with the weather condition. Among the four clusters, cluster No. 2 contains mainly the high loads acquired for the cooling load due to the water flow rate. The M_{CHW} plays an important role in determining the requirements of cooling load (Q_{CC}) at a certain temperature (ΔT_{CHW}). The variation of the operating input variables of each chiller has an impact on the output (Q_{CC}). For each cluster with operating conditions having similar characteristics, the MSE as fitness calculated in the analysis section. The effect of hot-humid weather condition for assessing cooling load based on T_{CHWR}. The inputs of T_{CHWR} has been re-adjusted by FSC-APSO approach. The satisfaction degree when the water flow set at a high value (20.134 kg/s), the chiller was performed with excellent comfort. Therefore, the behavior of cooling load based with a degree satisfaction, as given in Table 5.

Table 5. Cluster centers number after re-adjusting fuzzy logic rules

IF	ΔT_{CHW}	M_{CHW}	T_{AMB}	R_H	Then	Cooling demand	Satisfaction degree
if	MH	MH	MH	MH	***then***	Q_{CC1}	Good
if	ML	MH	ML	MH	***then***	Q_{CC2}	Excellent
if	MH	ML	ML	ML	***then***	Q_{CC3}	Poor
if	MH	ML	MH	MH	***then***	Q_{CC4}	Fair

The satisfaction degrees for cooling load demand Q_{CC} are good, excellent, poor, and fair, respectively, when we chose M_{CHW2}, the chiller is operated at 70% (0.7). Here, three scenarios in the chosen cluster implemented with different radius clusters. The first scenario termed as FSC-APSO1 was implemented when 'r_{a1}' set with 0.47. The second scenario termed as FSC-APSO2 conducted with 'r_{a2}' tuned to 0.43. The third scenario termed as FSC-APSO3 was carried out when 'r_{a3}' set to 0.51. Every cluster class is represented as a centre point of 'C_i'. Next, 'C_i' has been assigned to represent datasets and the particle vector for each C_i in the search space is restricted with a minimum and maximum scale. The change in the radius parameter has influenced on the difference between the potential 'C_i' and any data-point 'x_i'. The simulation was carried out based on output of those scenarios. The required cooling and energy usage to be calculated and they are executed with 4 clusters. Figure 10 depicts the cooling load and its usage of one chiller

4.0 Results and Discussion

4.1. Results

The main target of all scenarios is to adjust the flow rate of chilled water and its temperature difference to provide a comfortable level to reduce and maintain usage and cooling, respectively. The significance of M_{CHW} was used to quantify the change of to the variation of each operating C_{ij}. The flow rate of chilled water and its temperature plays a significant role to reduce energy consumption without compromising amount of cooling. The clustering input-output relation with a developed model for evaluating cooling load and its consumption as depicted in Figure 10. At 1st cluster, when scenario 1 was implemented, M_{CHW} and ΔT_{CHW} tuned with 18.191 kg/s and 6.32 °C respectively, then the chiller consumed and produced energy about 93.62 kW and cooling capacity of 480.8 kW. Energy consumption and cooling load both are depended on T_{CHWR} which has direct effect by weather condition. When T_{AMB} & R_H tuned to 32.66 °C & 63.44 %, respectively, T_{CHWR} is calculated to 12.8 °C. In scenarios 2 & 3, when the M_{CHW} tuned to (18.243, 18.287) kg/s and ΔT_{CHW} (6.37, 6.43) °C, chiller consumed (94.55, 95.59) kW and produced cooling of about (486.1, 491.8) kW, respectively. In this, energy and cooling both are depended on T_{CHWR}, which is calculated of about 12.85 and 12.91 °C, respectively. In cluster 1, both scenarios 2 & 3 consumed more energy due to the increase in T_{CHWR}. All scenarios result, after tuning M_{CHW} and ΔT_{CHW} is better than those basic models. At 2nd cluster, when scenario 1 was carried out, M_{CHW} and ΔT_{CHW} tuned to 20.134 kg/s and 6.18 °C respectively, here the chiller consumed and produced 100.87 kW of energy and 521.37 kW of cooling, respectively. Energy usage and cooling load are depending on T_{CHWR}. This T_{CHWR} has direct effect to the weather condition. When T_{AMB} and R_H tuned to 26.26 °C and 89.77 %, respectively, T_{CHWR} is calculated of about 12.67 °C. In scenarios 2 & 3, M_{CHW} increased to (20.347, 20.372) kg/s and ΔT_{CHW} tuned to (6.28, 6.31) °C. In this case, chiller consumed about (103.44, 103.95) kW in order to produce a chilled water capacity of (535.74, 538.67) kW. The consumption and cooling both are depended on T_{CHWR}, which is calculated of about 12.77 & 12.8 °C, respectively. Here, in cluster 2, both scenarios 2 & 3 consumed more energy than scenario 1, and this due to the increase in T_{CHWR}.

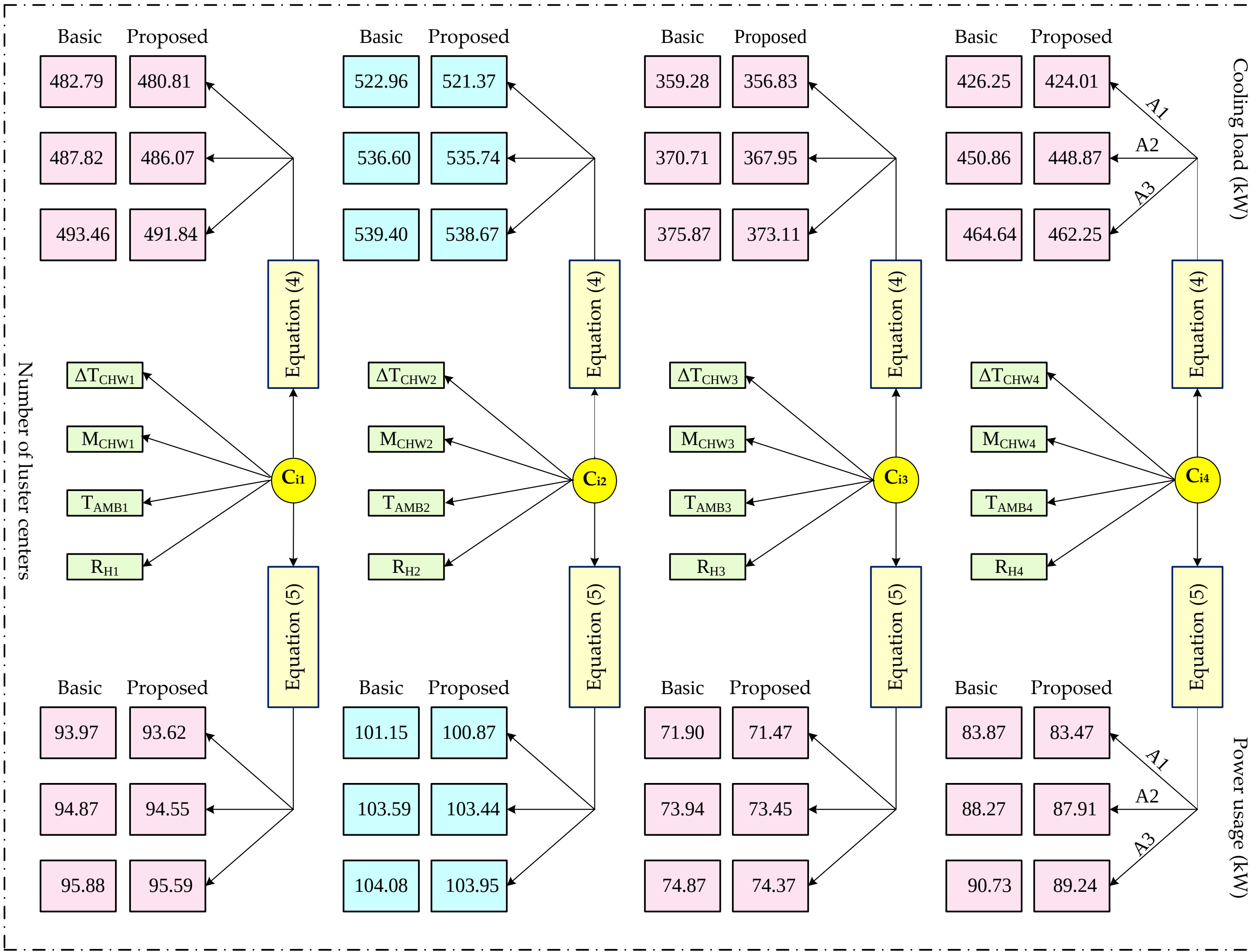

Figure 10. The clustering structural of cooling load and energy consumption

All scenarios result, after tuning M_{CHW} and ΔT_{CHW} is better than those basic models. At 3rd cluster, when scenario 1 was conducted, M_{CHW} and ΔT_{CHW} tuned with 12.69 kg/s and 6.75 °C, respectively. Here, chiller consumed 71.47 kW and produced cooling load capacity of 356.83 kW. Energy consumption and cooling load both are depended on 'T_{CHWR}' which has direct effect with T_{AMB} and R_H condition. When they tuned to 26.36 °C and 74.9 %, 'T_{CHWR}' is calculated to 12.67 °C. In scenarios 2 & 3, when M_{CHW} tuned to (13.27, 13.48) kg/s and ΔT_{CHW} (6.65, 6.64) °C, chiller consumed (73.45, 74.37) kW and produced cooling capacity of (367.95, 373.11) kW. Therefore, energy usage and cooling capacity both are depended on 'T_{CHWR}', which is calculated to 13.1 °C. Here, in cluster 3, both scenarios 2 & 3 consumed little bit more energy than scenario 1, due to the increase in T_{CHWR}.

All scenarios result, after tuning M_{CHW} and ΔT_{CHW} better than those basic models. At 4th cluster, when scenario 1 was implemented, M_{CHW} and ΔT_{CHW} tuned to 15.11 kg/s and 6.72 °C, respectively. Then, chiller consumed 83.47 kW and produced 424 kW of the chilled water capacity. Energy consumption and cooling load both are depended on T_{CHWR} which has direct effect to the weather condition. When T_{AMB} and R_H tuned to 29.11 °C and 79.27 %, respectively, T_{CHWR} is calculated of about 13.18 °C. In scenarios 2 & 3, when M_{CHW} and ΔT_{CHW} tuned to (15.82, 16.48) kg/s and (6.79, 6.72) °C, respectively, chiller consumed about (87.91, 89.24) kW to produce chilled water capacity of (448.87, 462.25) kW. The energy consumption and cooling load both are depended on T_{CHWR}, which is calculated of about (13.26, 13.18) °C, respectively. Here, in cluster 4, both scenarios 2 & 3 consumed little bit more energy than scenario 1. All scenarios result, after tuning temperature and flow rate of water better than those basic models as given in Table 6.

Table 6. Comparative results of cooling load and energy usage

Scenario 1			
Data-model	Actual data	Fundamental model	Proposed mode
Cooling load (kW)	545	523	521.4
Energy usage (kW)	112	101.2	100.9
Water flow (m3/h)	73.5	73.5	71.91
Scenario 2			
Data-model	Actual data	Fundamental model	Proposed model
Cooling load (kW)	545	536.6	535.7
Energy usage (kW)	112	103.6	103.4
Water flow (m3/h)	73.5	73.5	72.67
Scenario 3			
Data-model	Actual data	Fundamental model	Proposed model
Cooling load (kW)	545	539.4	538.6
Energy usage (kW)	112	104.1	103.9
Water flow (m3/h)	73.5	73.5	72.76

For the investigation, the highest cluster point was selected to evaluate the behavior of cooling performance. It was noticed that cluster 2 showed a less energy usage without compromising cooling load. From the results, the cooling load varied from 521.4 kW to 538.6 kW with all scenarios. This variation in cooling load and energy consumption is because of an increase/decrease the flow rate of chilled water and its temperature.

4.2. Discussion and Analysis

We observed, M_{CHW} and ΔT_{CHW} restricted between (20.134 – 20.372) kg/s and (6.19 – 6.31) °C to produce cooling between (521 – 538) kW and increase electricity from (101 – 104) kW when implement FSC-APSO1, FSC-APSO2, and FSC-APSO3. The FSC-APSO 1 showed the superiority in comparison with the basic models. It achieved a reduction in energy consumption without compromising cooling demand. Table 5 depicts the actual data, basic, and proposed model. The mean absolute error (MAE), mean square error (MSE), and accuracy indicate to the fitness of the proposed technique. Thus, MAE, MSE, and Accuracy can be expressed as,

$$MAE = \frac{1}{k}\sum_{k=1}^{k=4}(T_{CHWR}^{Simulated} - T_{CHWR}^{Nominal}) \tag{16}$$

$$MSE = \frac{1}{k}\sum_{k=1}^{k=4}(T_{CHWR}^{Simulated} - T_{CHWR}^{Nominal})^2 \tag{17}$$

$$Accuracy = (1 - MSE) * 100\% \tag{18}$$

FSC-APSO fulfilled the requirements of cooling demand with a less MAE of about 0.4634 compared to other techniques. In addition, the proposed model has achieved a reduction in energy consumption of 10 %. It reduced energy consumption without compromising cooling load demand. To simplify the analysis, MAE, MSE, and accuracy are considered for each potential cluster depicted in Table 7. The data has been tested for operating chiller under partial load of 70 % as selected from the obtained data in Figure 2(a). The chiller consumed about 112 kW for a production of about 545 kW of chilled water capacity. When chiller performed at 70 % of the total load, the chilled water has a flow rate of 20.58 kg/s. In scenario 1 energy-reduced by 10 % of total energy consumption compared to the basic model. In scenario 2, energy-reduced by 7.7 % of the total energy consumption compared to the basic model. While in scenario 3, energy-reduced by 7.2 % of the total energy consumption compared to the basic model. In all scenarios and basic models, the chilled water capacity has met the requirements of cooling load demand. The demand kept consistently between 521.4 to 538.7 kW with a chilled water flow of (20.13 to 20.37) kg/s, respectively. As a result, scenario 1 outperformed in terms of energy reduction and it saved about 10 % of total energy consumption compared to the other cases. For analysis, MSE in Equation (00) has used as a fitness function to evaluate the performance of the proposed scenarios. Due to tuning the cluster radius, FSC-APSO1 achieved the least MSE of 0.27 compared to the basic model which has a big error of about 0.3. FSC-APSO1 has an MSE of 0.28 and a basic model of 0.32, FSC-APSO3 has an MSE of 0.27 and the basic model of 0.3. Here, FSC-APSO1 and FSC-APSO3 have the same MSE which is good, while the FSC-APSO3 consumed more energy. The FSC-APSO1 and FSC-APSO3 techniques have improved the accuracy of both 73.1 % compared to FSC-APSO2 of 71.6 % and the basic model ranged between 68.3 % and 69.8 %. Therefore, the FSC-APSO1 fulfilled the requirements of cooling demand and less energy consumption with an accuracy of about 73.1 % and MSE of 0.27

Table 7 Output clusters of T_{CHWR} model and analysis

Scenario No. 1	Nominal data	Basic model	Proposed model	Basic error	Proposed error
C_{1j}: (C_{11}, C_{12}, C_{13}, C_{14})	12.5	12.8236	12.7979	0.3236	0.2976
C_{2j}: (C_{21}, C_{22}, C_{23}, C_{24})	12.5	12.6887	12.6699	0.1887	0.1699
C_{3j}: (C_{31}, C_{32}, C_{33}, C_{34})	12.5	13.2469	13.2009	0.7469	0.7009
C_{4j}: (C_{41}, C_{42}, C_{43}, C_{44})	12.5	13.2205	13.1853	0.7205	0.6853
MAE	--	--	--	**0.4949**	**0.4634**
MSE	--	--	--	**0.3043**	**0.2696**
Accuracy	--	--	--	**69.6 %**	**73.1 %**
Scenario No. 2	Nominal data	Basic model	Proposed model	Basic error	Proposed error
C_{1j}: (C_{11}, C_{12}, C_{13}, C_{14})	12.5	12..8712	12.8477	0.3712	0.3477
C_{2j}: (C_{21}, C_{22}, C_{23}, C_{24})	12.5	12.7836	12.7736	0.2836	0.2736
C_{3j}: (C_{31}, C_{32}, C_{33}, C_{34})	12.5	13.1541	13.0146	0.6541	0.6046
C_{4j}: (C_{41}, C_{42}, C_{43}, C_{44})	12.5	13.2892	13.2592	0.7892	0.7592
MAE	--	--	--	**0.5245**	**0.4962**
MSE	--	--	--	**0.3172**	**0.2844**
Accuracy	--	--	--	**68.3 %**	**71.6 %**
Scenario No. 3	Nominal data	Basic model	Proposed model	Basic error	Proposed error
C_{1j}: (C_{11}, C_{12}, C_{13}, C_{14})	12.5	12.9294	12.9082	0.4294	0.4082
C_{2j}: (C_{21}, C_{22}, C_{23}, C_{24})	12.5	12.8081	12.7995	0.3081	0.2995
C_{3j}: (C_{31}, C_{32}, C_{33}, C_{34})	12.5	13.1441	13.0954	0.6441	0.5954
C_{4j}: (C_{41}, C_{42}, C_{43}, C_{44})	12.5	13.2161	13.1815	0.7161	0.6815
MAE	--	--	--	**0.5244**	**0.4962**
MSE	--	--	--	**0.3017**	**0.2688**
Accuracy	--	--	--	**69.8 %**	**73.1 %**

Due to tuning the cluster radius, FSC-APSO1 achieved the least MSE of 0.27 compared to the basic model which has a big error of about 0.3. FSC-APSO1 has an MSE of 0.28 and a basic model of 0.32, FSC-APSO3 has an MSE of 0.27 and the basic model of 0.3. Here, FSC-APSO1 and FSC-APSO3 have the same MSE which is good, while the FSC-APSO3 consumed more energy. The FSC-APSO1 and FSC-APSO3 techniques have improved the accuracy of both 73.1 % compared to FSC-APSO2 of 71.6 % and the basic model ranged between 68.3 % and 69.8 %. Therefore, scenario No. 1 (FSC-APSO1) fulfilled the requirements of cooling demand and less energy consumption with an accuracy of 73.1 % and MSE of 0.27. The fitness function termed as MSE and the accuracy of the algorithm scenarios are depicted in Figure 11. The 1st and 3rd scenarios have good results in terms of accuracy and MSE. Overall, in terms of maintaining load demand all scenarios have good results, while for reducing energy consumption, the 1st scenario is the best among other scenarios and basic model.

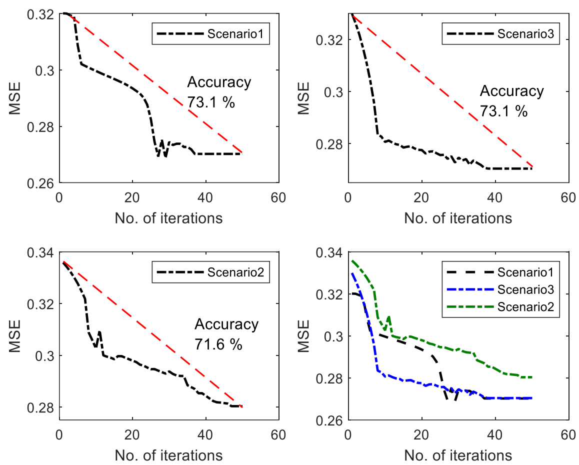

Figure 11. Fitness function (MSE) of algorithm scenarios and accuracy

5.0 Conclusions

The work presented used an optimized clustering technique to achieve the satisfaction of cooling load and reduction in energy usage. A proposed model considered the impact of weather parameters to assess to evaluate the output cooling behavior in a chiller plant. The data have used the clustering data based FSC optimized by APSO to tune the parameters of the FSC algorithm. Three scenarios by FSC-APSO algorithm was carried out with 4 inputs data. The fuzzy rules have been tuned by FSC to modify the rules centroid and APSO was used to minimize fuzzy rules error. MAE was used as a fitness function for evaluating the performance of FSC-APSO scenarios by tuning the parameter of clustering radiuses. The output of the clustering data using FSC-APSO scenarios were conducted in the proposed model. The obtained results met cooling demand requirements and reduced energy of about 10 % of the total energy consumption after optimized the parameters of chilled water systems. Considering the weather data assisted to select the best clusters to manage the wasted chilled water, it saved 33 m^3/h (9.24 kg/s) each chiller. Furthermore, the proposed has good accuracy of 73.1 % with a less MSE of 0.27 compared to the basic and existing system.

Acknowledgements

The authors would like to thank Latexx Manufacturing Company Sdn Bhd, Perak, Malaysia for providing data and tools, and all authors have read this manuscript. Also, the authors would like to express their gratitude to the Kampala International University (KIU), Uganda and UTP, Malaysia, University of Bahri, Sudan.

Declaration of conflict of interest

There is no conflict of interest of authors.

Appendix A

In this section, the fundamental mathematical models are explained; cooling load demand and its electricity consumption based on the water flow rate. For m^{th} chiller ($m = 1, 2, \ldots, M$), the operation mode γ_m can express in two conditions as given in,

$$\gamma_m = \begin{cases} 1, & when\ m^{th} chiller\ is\ ON \\ 0, & when\ m^{th} chiller\ is\ OFF \end{cases} \tag{19}$$

The cooling load (Q_W) that is produced by chillers in order to maintain the load demand, it can express as (Abdalla et al., 2016),

$$Q_{CC} = 4.197\gamma_{m(0,1)} \sum_{m=1}^{M} M_{CHWm}(T_{CHWR} - T_{CHWS}) \tag{20}$$

where M_{CHW} is the flow rate of chilled water, T_{CHWR} and T_{CHWS} are return and supply temperatures of chilled water, respectively. The energy consumption mainly depends on the chilled water temperature (Deng et al., 2015). Thus, it can be expressed as,

$$P_E = 0.75 * \gamma_m \left[\sum_{m=1}^{M} \sum_{t=1}^{T} M_{CHWm} (T_{CHWR} - T_{CHWS}) + 7.7 \right] \tag{21}$$

These fundamental models are assessed by clustering points in appendix B, and then compares with the proposed.

Appendix B

This section is described the outcome of dataset clustering. Table 8 gives the cluster points and standard deviation of each MF using FSC-APSO1. Table 9 shows the cluster points and standard deviation of each MF using FSC-APSO2. Table 10 depicts the cluster points and the standard deviation of each MF using FSC-APSO algorithm.

Table 8. The cluster centers and standard deviations of 4 inputs using FSC-APSO1

C_{ij}, σ_{ij}	Input1 ΔT_{CHW} (°C)	Input2 M_{CHW} (kg/s)	Input3 T_{AMB} (°C)	Input4 R_H (%)	Target T_{CHWR} (°C)
$\{C_{i1}, \sigma_{i1}\}$	6.3236, 0.9101	18.191, 2.5515	32.659, 1.9490	85.642, 5.9568	12.80
$\{C_{i2}, \sigma_{i2}\}$	6.1887, 1.0925	20.134, 2.8096	26.258, 1.4676	89.766, 5.7366	12.67
$\{C_{i3}, \sigma_{i3}\}$	6.7469, 0.1467	12.688, 3.1504	26.367, 0.6874	74.895, 5.4492	13.20
$\{C_{i4}, \sigma_{i4}\}$	6.7205, 0.9759	15.112, 3.0501	29.112, 1.4856	79.266, 6.1129	13.18

Table 9. The cluster centers and standard deviations of 4 inputs using FSC-APSO2

C_{ij}, σ_{ij}	Input1 ΔT_{CHW} (°C)	Input2 M_{CHW} (kg/s)	Input3 T_{AMB} (°C)	Input4 R_H (%)	Target T_{CHWR} (°C)
{C_{i1}, σ_{i1}}	6.3712, 1.0351	18.243, 2.5783	32.807, 2.0038	85.857, 6.0342	12.91
{C_{i2}, σ_{i2}}	6.2836, 1.1201	20.347, 2.6944	26.157, 1.3259	90.878, 5.7568	12.77
{C_{i3}, σ_{i3}}	6.6541, 0.1796	13.274, 2.8881	26.346, 1.0107	75.458, 5.4618	13.10
{C_{i4}, σ_{i4}}	6.7892, 1.0283	15.823, 3.2241	28.531, 1.4292	80.589, 5.9576	13.26

Table 10. The cluster centers and standard deviations of 4 inputs using FSC-APSO3

C_{ij}, σ_{ij}	Input1 ΔT_{CHW} (°C)	Input2 M_{CHW} (kg/s)	Input3 T_{AMB} (°C)	Input4 R_H (%)	Target T_{CHWR} (°C)
{C_{i1}, σ_{i1}}	6.4294, 1.0150	18.287, 2.8930	32.749, 2.0170	86.012, 5.8258	12.91
{C_{i2}, σ_{i2}}	6.3081, 1.1120	20.372, 2.7700	26.047, 1.3896	91.012, 6.0400	12.77
{C_{i3}, σ_{i3}}	6.6441, 0.2053	13. 479, 3.1106	26.535, 0.7869	75.854, 5.5514	13.80
{C_{i4}, σ_{i4}}	6.7161, 0.9692	16.484, 2.6514	28.698, 1.3342	81.016, 5.9830	13.18

References

ABDALLA, E. A. H. (2020). *MODELING AND OPTIMIZATION OF THE INDUSTRIAL PLANT USING ARTIFICIAL INTELLIGENT TECHNIQUES.* Universiti Teknologi PETRONAS.

Abdalla, E. A. H., Kumar, M., Abdalla, I. I., Mohamed, S. E. G., Soomro, A. M., Irfan, M., . . . Nowakowski, G. J. I. A. (2023). Modeling and Optimization of Isolated Combined Heat and Power Microgrid for Managing Universiti Teknologi PETRONAS Energy.

Abdalla, E. A. H., Nallagownden, P., Nor, N. M., Romlie, M. F., Abdalsalam, M. E., & Muthuvalu, M. S. (2016). *Intelligent approach for optimal energy management of chiller plant using fuzzy and PSO techniques.* Paper presented at the 2016 6th International Conference on Intelligent and Advanced Systems (ICIAS).

Chong, C., Ni, W., Ma, L., Liu, P., & Li, Z. (2015). The use of energy in Malaysia: Tracing energy flows from primary source to end use. *Energies, 8*(4), 2828-2866.

Deng, K., Sun, Y., Li, S., Lu, Y., Brouwer, J., Mehta, P. G., . . . Chakraborty, A. (2015). Model predictive control of central chiller plant with thermal energy storage via dynamic programming and mixed-integer linear programming. *IEEE Transactions on Automation Science and Engineering, 12*(2), 565-579.

Fong, S., Wong, R., & Vasilakos, A. V. J. I. t. o. s. c. (2015). Accelerated PSO swarm search feature selection for data stream mining big data. *9*(1), 33-45.

Hamid Abdalla, E. A., Nallagownden, P., Mohd Nor, N. B., Romlie, M. F., & Hassan, S. M. J. E. (2018). An application of a novel technique for assessing the operating performance of existing cooling systems on a university campus. *11*(4), 719.

Hamid, E., Nallagownden, P., Nor, N. B. M., & Muthuvalu, M. A. (2014). *Intelligent demand side management technique for industrial consumer.* Paper presented at the 2014 5th International Conference on Intelligent and Advanced Systems (ICIAS).

Lee, W.-S., Chen, Y. T., & Wu, T.-H. (2009). Optimization for ice-storage air-conditioning system using particle swarm algorithm. *Applied Energy, 86*(9), 1589-1595.

Maiolo, M., Mendicino, G., Pantusa, D., & Senatore, A. J. W. (2017). Optimization of drinking water distribution systems in relation to the effects of climate change. *9*(10), 803.

Mala-Jetmarova, H., Sultanova, N., & Savic, D. J. W. (2018). Lost in optimisation of water distribution systems? A literature review of system design. *10*(3), 307.

Nallagownden, P., Abdalla, E. A. H., & Nor, N. M. (2020). Power Consumption Optimization for the Industrial Load Plant Using Improved ANFIS-Based Accelerated PSO Technique *Practical Examples of Energy Optimization Models* (pp. 35-51): Springer.

Nallagownden, P., Abdalla, E. A. H., Nor, N. M., & Romlie, M. F. (2017). *Optimal chiller loading using improved particle swarm optimization.* Paper presented at the 9th International Conference on Robotic, Vision, Signal Processing and Power Applications.

Patterson, M. K. (2008). *The effect of data center temperature on energy efficiency.* Paper presented at the Thermal and Thermomechanical Phenomena in Electronic Systems, 2008. ITHERM 2008. 11th Intersociety Conference on.

Radeerom, M., & Tharathanmathikorn, K. (2015). *Intelligent system based supervision for energy management of water chiller plant*. Paper presented at the 2015 12th International Conference on Electrical Engineering/Electronics, Computer, Telecommunications and Information Technology (ECTI-CON).

Rezeka, S. F., Attia, A.-H., & Saleh, A. M. J. A. E. J. (2015). Management of air-conditioning systems in residential buildings by using fuzzy logic. *54*(2), 91-98.

Shaikh, P. H., Nor, N. B. M., Sahito, A. A., Nallagownden, P., Elamvazuthi, I., & Shaikh, M. (2017). Building energy for sustainable development in Malaysia: A review. *Renewable and Sustainable Energy Reviews, 75*, 1392-1403.

Siddiqi, U. F., & Sait, S. M. J. I. A. (2017). A new heuristic for the data clustering problem. *5*, 6801-6812.

Yi-Ling, H., Hai-Zhen, M., Guang-Tao, D., & Jun, S. J. A. i. c. c. r. (2014). Influences of urban temperature on the electricity consumption of Shanghai. *5*(2), 74-80.